https://doi.org/10.5194/gmd-2020-254
Preprint. Discussion started: 12 October 2020

Geoscientific Model Development Discussions
Open Access

Using a single column model (SGRIST1.0) for connecting model physics and dynamics in the Global-to-Regional Integrated forecast SysTem (GRIST-A20.8)

Xiaohan Li, Yi Zhang, Xindong Peng*, and Jian Li

State Key Laboratory of Severe Weather, Chinese Academy of Meteorological Sciences, Beijing, China, 100081

*CA: Xindong Peng, Email: pengxd@cma.gov.cn, Tel:+86 10 68409552

Abstract

A single column model (SGRIST1.0) is developed as a tool for coupling a full-physics package (from Community Atmosphere Model, version 5 (CAM5)) to the Global-to-Regional Integrated forecast System (GRIST). In a two-step approach, the full-physics package is first isolated and coupled to SGRIST1.0 for reducing the uncertainties associated with model physics and assessing its behavior, then assimilated by the model dynamical framework. In the first step, SGRIST1.0 serves as a tool for evaluating the physical parameterization suite in the absence of 3D dynamics. Three single column model test cases, including the tropical deep convection, shallow convection, and stratocumulus, demonstrate that the parameterization suite mimics the behaviors in the observations and the reference model (SCAM) outputs. Cloud fraction, cloud liquid, and some other micro- and macro-physical variables are sensitive to the model time step, suggesting time-step dependency of the corresponding parameterization schemes. The second step couples the physics package to the 3D dynamical modeling system, and the verified parameterization suite works well in GRIST. Two physics-dynamics coupling strategies are examined and found to have a clear impact on the intensity of the simulated storm. The incremental operator splitting strategy (ptend_f1_f1), produces a weaker storm than the pure operator splitting strategy (ptend_f2_sudden). Comparing these two splitting approaches, the ptend_f2_sudden coupling strategy has higher large-step stability than the ptend_f1_f1 option, but the intensity of the simulated storm is substantially reduced by ptend_f2_sudden provided that the time step becomes quite large. Some detailed model configuration strategies are suggested when using the CAM5 parameterization suite in GRIST.

https://doi.org/10.5194/gmd-2020-254
Preprint. Discussion started: 12 October 2020

Geoscientific Model Development Discussions

1. Introduction

Atmospheric general circulation models (AGCMs) have been widely used for weather forecasting and climate modeling. With the rapid development of computer architectures, the use of the quasi-uniform grid has become a popular strategy to escape from the pole problem that plagues the global models. A variety of such models have been developed or under ongoing development over the years (cf., Ullrich et al., 2017; Yu et al., 2019). Broadly speaking, an AGCM contains two major components, a dynamical core to solve the adiabatic resolved-scale fluid dynamics, and a physical parameterization suite for estimating the collaborative effects of the subgrid-scale dynamics and non-dynamical processes. In the most straightforward way, an AGCM can be formed by coupling these two components together. However, as Rome is not built in a day, the practice of model development is often done in a hierarchical manner.

As discussed in Reed and Jablonowski (2012), such a hierarchy typically starts from a 2D shallow-water model, then to a 3D hydrostatic or nonhydrostatic dry dynamical core with vertical extension, and to a moist AGCM with model physics. The dry dynamical core can be evaluated with a series of benchmark test cases (e.g., Jablonowski et al., 2008; Ullrich et al., 2012). Most of these test cases are short-term deterministic experiments that focus on the quantitative assessment of numerical performance. An AGCM coupled with a full physical parameterization suite can be evaluated with the aqua-planet experiments (APEs) (Neale and Hoskins, 2000; Blackburn et al., 2013), and/or the Atmospheric Model Intercomparison Project (AMIP) (Gates, 1992; Gates et al., 1999). The APEs allow full physics-dynamics interaction in an AGCM with simplified surface boundary conditions. The APEs focus on statistical behavior of the model climate, thus no analytical solution is available. The APE runs are usually evaluated by qualitative analysis or comparison with other model outputs. The AMIP experiments further require the AGCMs to be forced by realistic geography and boundary conditions. Such simulations are usually evaluated against the global reanalysis data or via model intercomparison. Identification and interpretation of the model errors in the APE and AMIP experiments depend on the dynamics, physics, and the nonlinear interaction between them, all of which may introduce uncertainty that hinders the understanding of the model behaviors.

There is therefore a gap from the pure model dynamics to the full-fledged AGCM. The use of the simplified physics packages has been suggested to bridge this gap. For example, Reed and Jablonowski

(2012) used an intermediate complex parameterization suite to study the role of manifold dynamical cores in tropical cyclone evolution. A climate extension of this physics package was further presented by Thatcher and Jablonowski (2016). Such test cases drive the dynamical model towards some well-expected behaviors, thus helping to disentangle the impact of dynamics and its coupling to physics in a moist environment, and facilitate the model development and performance understanding (Zhang et al., 2020). From the perspective of model development however, direct coupling of a full parameterization suite to the model dynamics still has a gap in that the physics package itself may introduce additional uncertainties. This issue becomes especially intricate when a sophisticated physics package is ported to a completely different model system. In this regard, a single-column model (SCM) is a useful tool. It isolates the impact of the physics package and assesses its behavior in the absence of 3D dynamics, thus separating the physical effect from the dynamical one (Randall et al., 1996; 2003; Moncrieff et al., 1997; Neggers et al., 2012; Zhang et al., 2016).

The SCM focuses on the assessment of physics effects within a single vertical atmospheric column, owing to the 1D structure of most conventional parameterizations. Calculation of the grid-scale horizontal advection in the model dynamics is replaced by observational or analysis data. Therefore, the SCM is able to provide rapid feedback when coupling a full parameterization suite to a model, and is computationally cheaper than the global AGCM runs (Neggers, 2015; Zhang et al., 2016). Many modeling groups have developed their SCMs as a necessary branch of the AGCMs for the evaluation of the parameterization schemes (Guo et al., 2014; Gettelman and Morrison, 2015; Gettelman et al., 2019). Evaluation of different physical parameterization schemes for a specific physical process, such as the cloud feedback on temperature and humidity, is enabled by SCM intercomparison (Klein et al., 2009; Zhang et al., 2013; Davis et al., 2013). The SCM may be considered as a configuration of the simplified dynamical component and the entire parameterization suite.

In this study, we demonstrate that a SCM can be used at the early stage of model development for connecting model dynamics and physics. It serves as a bridge for physics-dynamics coupling (PDC), and facilitates the evaluation of dynamics-physics interaction at reduced uncertainty. Following the above-mentioned strategy, the parameterization suite of Community Atmosphere Model, version 5 (CAM5) has been coupled to the Global-to-Regional Integrated forecast System (GRIST). In a two-step approach, we first isolate the CAM5 parameterization suite and evaluate its performance with the

https://doi.org/10.5194/gmd-2020-254
Preprint. Discussion started: 12 October 2020

aid of the SCM, then we couple the validated parameterization suite to a previously established dynamical modeling system (Zhang et al., 2020). It is emphasized that the work here is not to port the GRIST dynamics to the CAM5 framework, for which case the uncertainties mainly result from the model dynamics and its coupling to physics, thus using a SCM would be less useful. Both the short-term deterministic test and the long-term climate test on an aqua-planet have been performed to further evaluate and understand the behaviors of the CAM5 package within the different model systems. Two PDC strategies are evaluated with an idealized tropical cyclone test case. This test has been previously investigated by Li et al. (2020) for evaluating the impact of PDC on time-step sensitivity in the full-physics CAM5, and by Zhang et al. (2020) for understanding the behaviors of different PDC strategies in the simple-physics GRIST. Long-term climate modeling in a standard APE configuration is also evaluated, and the results are compared against the simulation of CAM5 with the finite-volume dynamical core (CAM5-FV; Lin, 2004; Neale et a. 2010), as well as other model results available in the literature (cf., Blackburn et al., 2013).

This paper is structured as follows. Section 2 briefly reviews the GRIST framework, then introduces the development of the SCM (referred to as SGRIST1.0). A brief description of the CAM5 parameterization suite is also presented in Section 2. Evaluation of the physics-dynamics coupled SGRIST1.0 via three test cases is shown in Section 3. Section 4 presents the 3D modeling of GRIST on an aqua-planet, where an idealized tropical cyclone experiment and long-term APE simulations are conducted to assess full physics-dynamics interaction. Finally, Section 5 presents a summary.

2. Single column model and the CAM5 physics package

2.1 GRIST and its SCM formulation

The GRIST framework is developed for exploring a unified weather and climate modeling system. The dry dynamical core (dycore)[1] is formulated on a horizontal unstructured C-grid, using the methods proposed in Thuburn et al. (2009) and Ringler et al.(2010), with improved vorticity flux (Zhang 2018). A third-order flux operator (Skamarock and Gassmann, 2011) is used for scalar and vorticity transport on the Voronoi and Delaunay mesh (cf., Zhang, 2018; Zhang et al., 2019). The explicit third-order Runge-Kutta scheme (Wicker and Skamarock, 2002) is used for time integration. The dry-mass coordinate allows a flexible switch between the hydrostatic and nonhydrostatic solvers,

[1] For GRIST, dycore is specifically referred to the part of governing equations without tracer transport. This should be distinguished from the typical definition of dynamical core in a broad sense.

https://doi.org/10.5194/gmd-2020-254
Preprint. Discussion started: 12 October 2020

and a vertically layer-averaged treatment is used (Zhang et al., 2019). The time-averaged normal mass flux is used to couple tracer transport to the dycore. The tracer transport feeds back the moisture constraint tendencies to the dycore at each tracer time step. (Zhang et al., 2020). The dynamical component of GRIST has been extensively assessed based on various benchmark test cases (Zhang 2018; Zhang et al., 2017; 2019; 2020; Wang et al., 2019). A tailored model physics package can be used by the GRIST framework as a plugin, and the results from a suite of simple physics have been examined (Zhang et al., 2020).

SGRIST1.0 has its own top driver whose workflow is independent from the 3D model. The dynamical component of the SGRIST1.0 is reduced to handle vertical advection within a single atmospheric column. The governing equations are formulated in a pressure coordinate, basically similar to those in Zhang et al. (2016):

$$\frac{\partial T}{\partial t}=(\frac{\partial T}{\partial t})_{phys}-(\vec{V}\cdot\nabla T)_{LS}-\omega_{LS}\frac{\partial T}{\partial p}+\frac{R_d T}{pc_p}\frac{dp}{dt}+[(T-T_{obs})\frac{dt}{d\tau}]_{rex}, \qquad (1)$$

$$\frac{\partial q}{\partial t}=(\frac{\partial q}{\partial t})_{phys}-(\vec{V}\cdot\nabla q)_{LS}-\omega_{LS}\frac{\partial q}{\partial p}+[(q-q_{obs})\frac{dt}{d\tau}]_{rex}, \qquad (2)$$

where T and q are temperature and specific humidity; p and ω are pressure and pressure vertical velocity; R_d represents gas constant for dry air, and c_p the heat capacity at constant pressure for dry air; subscript *phy* denotes the physical parameterizations, *LS* stands for large-scale fields, *rex* represents relaxation terms, and *obs* stands for observational data. Here $d\tau$ is the time scale of relaxation. SGRIST1.0 predicts temperature and humidity using the prescribed large-scale horizontal tendencies as forcing terms, together with the subgrid-scale tendencies provided by the parameterization suite. The time integration method and the vertical transport are the same as that in the 3D model dynamics. The approximation of T and q values at the interface follows the standard line-based third-order flux operator in Wicker and Skamarock (2002),

$$q_{k+\frac{1}{2}}=\frac{7}{12}(q_{k+1}+q_k)-\frac{1}{12}(q_{k+2}+q_{k-1})+sign(\omega_{k+\frac{1}{2}})\frac{1}{12}[(q_{k+2}-q_{k-1})-3(q_{k+1}-q_k)]. \qquad (3)$$

Equation (3) gives the approximation of q as an example, in which subscript k represents vertical layer index, and k+1/2 stands for the level of the interface. The large-scale forcing terms and initial conditions are derived from an Intensive Observation Period data set (IOP). Momentum, pressure

https://doi.org/10.5194/gmd-2020-254
Preprint. Discussion started: 12 October 2020

vertical velocity, and surface pressure at each integration step are also provided by the IOP data. SGRIST1.0 does not predict additional advective tendencies for prognostic variables other than temperature and specific humidity, i.e., cloud liquid, cloud ice, and the related number concentrations are only governed by the physical parameterizations. For the 3D model, these values will be advected by the tracer transport module (cf., Zhang et al., 2020).

2.2 The CAM5 physical parameterization suite

The CAM5 physical parameterization suite contains the Zhang–McFarlane deep convection scheme (Zhang and McFarlane, 1995; Neale et al., 2008), the University of Washington shallow cumulus scheme and moist boundary layer turbulence scheme (Park and Bretherton, 2009; Bretherton and Park, 2009), the Morrison–Gettelman microphysics scheme and the Park macrophysics scheme to deal with the stratiform cloud properties (Morrison and Gettelman, 2008; Park et al., 2014). The RRTMG software is used to calculate short- and longwave radiation (Iacono et al., 2008). The default values of the physics parameters follow the 1.0°-resolution CAM5 model configuration (Neale et al., 2010). Besides, an ocean surface flux scheme is used to provide latent heat flux, sensible heat flux, and momentum flux at sea surface at each step. The effect of prognostic aerosols on micro- and macrophysics and radiation is not considered in this study. The physical parameterizations are coupled to SGRIST1.0 using an operator splitting approach, as the ptend_f2_sudden in the 3D dynamics (Zhang et al., 2020). Each physical parameterization is sequentially calculated in the same order as that in CAM5.

3. Performance of SGRIST

We select three SCM test cases, designed to simulate tropical convection, shallow convection, and stratocumulus over the ocean, to demonstrate the coupling of the CAM5 physics package to the GRIST framework. The simulations of SGRIST are compared with the SCM of CAM5 (SCAM, Hack and Pedretti, 2000) and the IOP data. SCAM uses the Eulerian scheme to calculate the vertical advection of temperature, and a semi-Lagrangian method to handle the vertical advection of moisture variables. The physical parameterizations used in SCAM are the same as those in SGRIST1.0. To exclude possible influences of vertical resolution, all simulations in SCAM and SGRIST1.0 are run at the same 30 vertical levels.

We first conduct the Tropical Warm Pool International Cloud Experiment (TWP-ICE, May et al.,

https://doi.org/10.5194/gmd-2020-254
Preprint. Discussion started: 12 October 2020

2008) to evaluate the representation of tropical precipitation and cloud in SGRIST1.0. The TWP-ICE IOP forcing data set is derived from the observational data by Xie et al. (2010), which covers the period from 17 Jan. to 12 Feb. 2006 at a 3-hour time interval. Davis et al. (2013) indicated that the TWP-ICE experiment can be divided into two periods, the convection active period from 00Z 20 to 12Z 25 Jan. 2006, and the relatively suppressed period after 12Z 25 Jan. The 14-day simulation is initialized with the IOP data on 19 Jan. 2006. The model time step (denoted as *dt*) is set as 1200 s.

Figure 1 shows the time evolution of the precipitation rate of SGRIST1.0, SCAM, and IOP data. SGRIST1.0 and SCAM show consistent precipitation during both the convection active and suppressed periods. The modeled precipitation is close to the IOP data during the convection active period, while the peaks at 21, 23, and 24 Jan. are about 15 to 20 mm day^{-1} less than the IOP data. The difference of the diurnal variation between the modeled precipitation and the IOP data is evident during the convection suppressed period. As the dynamic forcing is much weaker during the suppressed period, the physical parameterizations exert a relatively stronger influence in comparison to the convection active period. It suggests that the physical parameterizations in SGRIST1.0 and SCAM display a very similar result in precipitation despite the dynamical components are different.

Representation of the midlevel moisture is very important for a model to correctly describe the cloud. The simulated relative humidity is consistent with the IOP data during the convection active period (Figure 2a). However, a notable difference, up to 20%, is observed between the simulated humidity and the IOP observation after the transition to the convection suppressed period. Davis et al. (2013) indicated that most of the SCMs reduce the humidity too much in the transition period compared with the IOP data and cloud-resolving models (see Figure 5 in Davis et al., 2013). We speculate that the poor performance of SCMs in simulating midlevel humidity during the transition period is a common deficiency as strong interaction among physical parameterizations is necessary for such a period. Figures 2b and 2c show the period-average of cloud fraction for the convection active period and suppressed period in simulations with *dt* = 1200 and 2400 s, respectively. Cloud fraction is quite sensitive to the time step, especially during the convection suppressed period, where the largest difference reaches 0.7 at about 200 hPa. The dynamical component of the SCM also impacts the modeled cloud fraction. A two-time-level third-order Runge-Kutta time integration scheme is used in SGRIST1.0, while a three time-level leapfrog integration scheme is adopted in SCAM. The vertical

https://doi.org/10.5194/gmd-2020-254
Preprint. Discussion started: 12 October 2020

advection schemes for specific humidity and the physics time step are therefore different between SGRIST1.0 and SCAM. SGRIST1.0 tends to predict less ice cloud at high levels (above 200 hPa) than SCAM during both the convection active and suppressed periods.

A shallow tropical trade cumulus case in the Barbados Oceanography and Meteorology Experiment (BOMEX) (Holland and Rasmusson, 1973; Siebesma et al., 2003) is used to evaluate SGRIST1.0 on modeling shallow cumulus. The BOMEX was observed to be remarkably steady without apparent precipitation or mesoscale circulation. The BOMEX simulation is a 6-hour run without relaxation. Figures 3a and 3b show a comparison of temperature and specific humidity profiles between the initial state and the SGRIST1.0 output averaged over the last 3 hours of simulation. Figure 4 compares the average cloud properties in the last 3-hour simulation using the SGRIST1.0 and SCAM with dt = 600, 1200, and 2400 s respectively. The shallow cumulus cloud is mainly concentrated at 950 hPa. The (cumulus) cloud fraction and updraft mass flux in the SGRIST1.0 simulation are consistent with those using half of the time step in SCAM since the physics time step in the three time-level leapfrog scheme of SCAM is twice of that in the two-time-level scheme of SGRIST1.0. Both the updraft mass flux and cumulus cloud fraction are in good agreement with the large-eddy simulation (LES) in Park and Bretherton (2009). The maximum of updraft mass flux decreases slightly with the model time step. It suggests that the model time step slightly influences the University of Washington shallow cumulus parameterization. Li et al. (2020) indicated that the time step sensitivity of shallow convection was attributable to the moist boundary layer turbulence. The sensitivity of cloud fraction and cloud liquid amount to the time step is also discernible in the BOMEX test case. A possible reason for the time step sensitivity lies in the stratiform cloud scheme, in which the macrophysics and microphysics are sequentially split. Macrophysics is the main source of cloud liquid water for microphysics. Gettelman et al. (2015) indicated that the forward-Euler time integration scheme was used in the microphysics parameterization, and a longer time step facilitates the depletion of cloud liquid, resulting in more condensation by macrophysics for the next time step. Additional sub-stepping for the stratiform cloud scheme will help reduce the sensitivity to time step.

A drizzling marine stratocumulus cloud case in the Dynamics and Chemistry of Stratocumulus II experiment, case RF02 (DYCOMS-RF02) (Stevens et al., 2003; Ackerman et al., 2009) is further examined. The DYCOMS-RF02 is an idealized test case of steady nocturnal stratocumulus under a

https://doi.org/10.5194/gmd-2020-254
Preprint. Discussion started: 12 October 2020

dry inversion with embedded pockets of drizzling open cellular convection. Profiles of the initial temperature and specific humidity from the IOP data and the time-average of SGRIST1.0 simulation are compared in Figures 3c and 3d. The DYCOMS-RF02 simulations are run for 15 hours with *dt* = 300, 600 and, 1200 s. Figure 5 shows the time-average of the moist physical properties over the last 5-hour simulations using the SGRIST1.0 and SCAM models, respectively. The low-level stratocumulus cloud is steady and concentrated in a layer between 900 and 950 hPa. The cloud fraction reaches 1 at 920 hPa. The cloud liquid, rain mass, and rain number are sensitive to the time step in SCAM, apart from being sensitive to vertical resolution as indicated in Gettelman et al. (2015). The rain mass and rain number concentration in SGRIST1.0 are less than those in SCAM at the corresponding time steps, and their sensitivity to time step is less discernible. The DYCOMS-RF02 test case in this study demonstrates the impact of the dynamical core, such as the time integration method of temperature and humidity, on the cloud fraction and other micro- and macrophysics characteristics, although the physics-dynamics interaction in a SCM is limited. It is suggested that these micro- and macrophysics variables are sensitive to the profile of humidity, which varies with the time integration method in the dynamical component.

4. 3D modeling with the CAM5 package (GRIST-CAM5phys)

4.1 Idealized tropical cyclone experiment on an aqua-planet

The three single-column test cases have provided a valuable evaluation of the isolated CAM5 parameterization suite. It verifies that the physics package behaves properly in an isolated configuration. The package is then transferred to the 3D GRIST model for further understanding the model behavior under full nonlinear physics-dynamics interaction.

The general PDC workflow of GRIST has been described in Zhang et al. (2020) for the purpose of global multiscale modeling applications. In this study, we focus on the coupling of the CAM5 package to the hydrostatic dynamical core. Gross et al. (2018) indicated that the PDC strategy, representing the way to exert physics tendencies on the model dynamics, had a great influence on the physics–dynamics interaction. Li et al. (2020) has demonstrated the effect of PDC strategies on the sensitivity to time step of the spectral element dynamical core in CAM5 (CAM5-SE). For GRIST, two PDC coupling options are investigated: ptend_f1_f1 and ptend_f2_sudden (see Zhang et al. 2020 for details). Ptend_f2_sudden is a pure operator splitting approach, which is also used in CAM5-FV.

https://doi.org/10.5194/gmd-2020-254
Preprint. Discussion started: 12 October 2020

Ptend_f1_f1 incrementally adds the physics tendencies to the dycore and the tracer transport, respectively. The difference between the ptend_f1_f1 and the dribbling strategy (se_ftype0) used in CAM5-SE is that ptend_f1_f1 treats the dycore and passive tracer transport as two separate components, while the dribbling approach treats them as a whole.

As in the simplified physics configuration (Zhang et al., 2020), an idealized tropical cyclone experiment (Reed and Jablonowski, 2011a) is used to examine the model behavior in comparison with the CAM5 model. Evolution of the storm highly resembles the weather processes with strong physics-dynamics interactions, providing a practical implication for the factual weather modeling. We first evaluate the behaviors of the moist model at different resolutions, then compare the impacts of different PDC strategies on physics-dynamics interaction.

The horizontal resolutions for the test cases are set to G6 (~120 km), G7 (~60 km), and G8 (~30 km). Table 1 shows the corresponding time step combinations at each resolution. The 10-day simulations are run at 30 vertical levels. Figure 6 and Figure S1 separately show the simulated storm at days 5 and 10 for the ptend_f2_sudden and ptend_f1_f1 configurations. The model time steps are 1200 s for G6, 600 s for G7, and 300 s for G8 resolutions. The storm in the ptend_f2 simulation shows a slightly northwestward drift with the increasing resolution. It also becomes more organized and more intense with the increasing resolution. At the highest resolution (G8), the maximum wind speed exceeds 80 m s^{-1} at about 900 hPa on day 10, showing a very strong tropical cyclone. The radius of the maximum wind (RMW) decreases slightly as the resolution increases, and the size of the RMW at G8 resolution is roughly 1.5°-2°. The storm in the ptend_f2_sudden simulation generally shows a similar dependence of size and intensity on resolution compared with the CAM5-FV (see Figures 3 and 6 in Reed and Jablonowski (2011b) for the CAM5-FV simulation at corresponding resolutions). At each resolution, the tropical cyclone evolves slightly more northward (less than 1°) in GRIST than that in CAM5-FV. The intensities of the storm on day 10 in GRIST-CAM5phys and CAM5-FV produces are highly consistent. The storm in ptend_f1_f1 simulation is less intense than that in ptend_f2_sudden by day 10 at each resolution, as evidenced by the less conspicuous vertical development of the storm in ptend_f1_f1. No discernable difference of location and size of the storm at days 5 and 10 is found between ptend_f1_f1 and ptend_f2_sudden simulations. The coupling approach mainly impacts the intensity of the simulated storm.

https://doi.org/10.5194/gmd-2020-254
Preprint. Discussion started: 12 October 2020

Geoscientific Model Development
Discussions

The full-physics test of GRIST shows that ptend_f2_sudden is more stable than ptend_f1_f1. Ptend_f2_sudden survives all the time step configurations listed in Table 1, while ptend_f1_f1 aborts at 2400 s at G7 resolution and 1200 s at G8 resolution. This is consistent with the conclusion suggested in Zhang et al. (2020) using the simplified parameterization suite. Figure 7 shows the path of the simulated storm center from day 2 to 10 in all the stable runs at G7 and G8 resolutions. The path of the storm varies slightly as the model time step changes in both ptend_f1_f1 and ptend_f2_sudden simulations. The maximum deviation of the storm location at day 10 among different time step simulations of ptend_f2_sudden is 3° in longitude at G7 resolution and 2.5° at G8 resolution. The storm evolves more westward at G8 resolution than at G7, except for the ptend_f2_sudden simulation with dt = 1200 s at G8. Overall, ptend_f2_sudden shows more consistent storm paths than ptend_f1_f1.

Figure 8 illustrates the temporal evolution of maximum wind speed at 850 hPa and the minimum surface pressure at G6, G7, and G8 resolutions. The model is perturbed using different physics time steps, and the results of CAM5 in such experiments can be found in Li et al. (2020). The maximum wind speed increases and the minimum surface pressure decreases with increasing resolution in both PDC configurations. The maximum intensity at each resolution has reached its peak around day 7 and slowly decay thereafter. The evolution of the storm intensity in GRIST at the lowest resolution is more consistent with that in higher resolutions, while in CAM5-FV, the storm does not fully develop over 10-day simulation at 1° resolution (see Figure 8 in Reed and Jablonowski, 2011b). The storm evolves more intensively in the ptend_f2_sudden configuration than in ptend_f1_f1. This is evidenced by both the higher maximum wind speed and the lower minimum surface pressure after day 7. In the ptend_f2_sudden cases, the maximum intensity on day 10 decreases more than 10 m s^{-1} when using the largest time steps at G7 (dt = 2400 s) and G8 (dt = 1200 s). This is also consistent with the earlier conclusion drawn based on the simple parameterization suite (see Figure 10 in Zhang et al., 2020). Therefore, a large time step (>2400 s at G7 resolution or >1200 s at G8) is not recommended in the GRIST-CAM5phys configuration. The model time step (when stability is ensured) in both ptend_f1_f1 and ptend_f2_sudden configurations has a much weaker impact on the storm intensity in comparison with the CAM5-SE with the dribbling coupling strategy (Li et al., 2020). This implies that the impact of the PDC strategy on the time step sensitivity has a close relationship with the model dynamics, i.e., such an issue is model dependent.

4.2 Climate simulation based on the standard Aqua-Planet experiment

In this section, we present the climate simulation of APE using the GRIST-CAM5phys model. The APE configuration follows Neale and Hoskins (2000). The CONTROL sea surface temperature (*SST*) distribution is given by,

$$SST = \begin{cases} 27[1-\sin^2(\frac{3\varphi}{2})], & -\frac{\pi}{3} < \varphi < \frac{\pi}{3}; \\ 0, & \text{otherwise}, \end{cases} \tag{4}$$

where φ is latitude. An idealized distribution of ozone based on the AMIP II climatology (Liang and Wang, 1996) is used. The simulation is run for 3.5 years with ptend_f2_sudden configuration at G6 with 30 vertical levels. The time steps for physics, tracer transport and dycore are 1800s, 900s, 300s, respectively. The analysis is conducted on the simulation of the last 3 years as proposed by Blackburn et al. (2013).

Figure 9a shows the comparison of time-zonal averaged total, convective, and large-scale precipitation between GRIST-CAM5phys and CAM5-FV. Both GRIST-CAM5phys and CAM5-FV exhibit a single inter tropical convergence zone (ITCZ). The most discernable difference of precipitation between GRIST and CAM5-FV occurs in the tropics. The tropical precipitation mainly occurs between 10° S and 10° N. The total precipitation over the equator reaches 24 mm day^{-1} in GRIST-CAM5phys and is 6 mm day^{-1} higher than that in CAM5-FV. This difference is attributed to the large-scale precipitation. The dynamical core has a more important impact on the large-scale precipitation than the convective precipitation. It suggests a tight interaction between the dynamical core and the stratiform parameterization as indicated by Herrington and Reed (2017). Blackburn et al. (2013) also showed a large variation of the tropical large-scale precipitation among the participated models in the APE. The maximum of time-zonal averaged convective precipitation in GRIST-CAM5phys is 14 mm day^{-1}, which is consistent with that in CAM5-FV.

The frequency-intensity relation provides more information regarding the rainfall properties. Figure 9b shows the frequency distribution of daily precipitation in the domain confined within 10° S and 10° N, with precipitation less than 0.5mm day^{-1} being omitted. The occurrence fraction decreases monotonically with the intensification of precipitation in both GRIST-CAM5phys and CAM5-FV. Below 30 mm day^{-1}, the convective precipitation occupies a greater fraction than the large-scale precipitation. The maximum value of convective precipitation is 70 mm day^{-1} and 120 mm day^{-1} in

GRIST-CAM5phys and CAM5-FV respectively. GRIST-CAM5phys has a greater fraction of large-scale precipitation occurring at rates less than 120 mm day^{-1} compared with CAM5-FV, and the extreme in GRIST-CAM5phys is about 100 mm day^{-1} less than CAM5-FV. The GRIST-CAM5phys and CAM5-FV show a similar propagation characteristic of the equatorial wave, as characterized by the precipitation field in Figure 10. The rain bands feature an eastward propagation with some smaller-scale rain cells propagating westward within the eastward propagating envelope. Such an eastward propagation feature is slightly more intense in CAM5-FV than that in GRIST-CAM5phys.

The zonal-time averaged temperature of GRIST-CAM5phys shown in Figure 11a is zonally symmetric as expected, and is very close to CAM5-FV and the multi-model mean in Blackburn et al. (2013). The difference of tropospheric temperature between the tropics and midlatitude is about 30 K and the maximum gradient of which is at 30° latitude. The temperature difference is reduced to less than 5 K between 60° latitude and the pole, associated with the zero gradient of SST profile in the APE. The specific humidity field (not shown) decreases with latitude and altitude, which is similar to the distribution of temperature. The narrow equatorial peak of humidity at mid-troposphere reflects the descent limb of Hadley circulation. Figures 11b and 11c show the time-zonal mean of zonal and meridional wind speed in GRIST-CAM5phys. The westerly jet core is as intense as 58 m s^{-1} and located at 30° latitude and upper troposphere (~200 hPa). The thermal wind balance is clearly established at midlatitude, as evidenced by the maximum vertical gradient of zonal wind speed being located at the same latitude with the maximum vertical gradient of tropospheric temperature. The meridional wind presents a three-cell circulation in each hemisphere, as typically found for an Earth-like atmosphere. The maximum wind speed in the low-level convergent flow of Hadley cell is about 0.5 m s^{-1} stronger compared with the multi-model mean (see Figure 3 in Blackburn et al., 2013). The eddy kinetic energy (Figure 11d) exhibits a similar pattern as in the simple physics test (see Figure 11 in Zhang et al., 2020), and the maximum magnitude (~400-~450 m^{2}s^{-2}) is also consistent with the results obtained by using the default Held-Suarez forcing in the dry and moist atmosphere (cf., Zhang et al., 2019; Zhang et al., 2020). These results demonstrate that GRIST-CAM5phys produce reasonable statistical behaviors under full physics-dynamics interaction.

5. Summary

As part of the model development efforts, this study developed a single column model

https://doi.org/10.5194/gmd-2020-254
Preprint. Discussion started: 12 October 2020

(SGRIST1.0) and uses it as a bridge for coupling a full model physics package to a new unstructured-mesh modeling system. We demonstrate that SGRIST1.0 can be an efficient tool for isolating sophisticated model physics and reducing its uncertainty during the transfer. Based on such a strategy, the CAM5 physics package has been separately evaluated in the absence of 3D dynamics, then successfully transferred to the GRIST framework.

During the development, SGRIST1.0 provides a helpful tool to rapidly detect code errors and bugs in an economic and efficient way. Three SCM test cases provide valuable evaluations of the CAM5 parameterization suite. Overall, SGRIST1.0 produces reasonable simulation results, which are consistent with SCAM under multiple scenarios including tropical convection, shallow convection, and stratocumulus. SGRIST1.0 simulates convective precipitation very close to the observation under strongly forced conditions. Details in the physical parameterizations exert a strong influence on precipitation when the forcing is weak. The cloud fraction, cloud liquid, and some other micro- and macrophysics variables are sensitive to the model time step, which implicates the time step sensitivity of the stratiform cloud scheme in CAM5 physics. The dynamical component of the single column model also has an impact on the micro- and macrophysics variables especially in the steady cases such as DYCOMS-RF02. These state variables might be sensitive to the profile of humidity which varies with the time integration method in the dynamical core.

The transferred physics package has been installed and evaluated in the 3D model (GRIST-CAM5phys). The idealized tropical cyclone test case shows that GRIST-CAM5phys behaves similarly to CAM5-FV. The storm evolves more intense and more organized as the resolution increases. In GRIST-CAM5phys, the pure operator splitting coupling strategy, ptend_f2_sudden, is more stable than the incremental operator splitting coupling strategy, ptend_f1_f1. Ptend_f2_sudden substantially reduces the intensity of the storm only when the model step becomes very large, consistent with the previous conclusion drawn from the simple physics configuration. According to the idealized tropical cyclone simulations, it suggests that the appropriate model time step should be less than 2400 s at G7 resolution and 1200 s at G8. Of course, more careful examinations are needed for realistic simulations to determine the maximum allowable time step at each resolution. The PDC strategy is found to have an impact on the intensity of the storm. The ptend_f1_f1 configuration produces a weaker storm than the ptend_f2_sudden configuration at G6-G8 resolutions. The effect of PDC strategies on the

https://doi.org/10.5194/gmd-2020-254
Preprint. Discussion started: 12 October 2020

sensitivity to time step is model dependent, as evidenced by the comparison between this study and the previous study using CAM5-SE (Li et al. 2020).

The climate simulation based on a standard APE shows a reasonable performance of the model under full physics-dynamics interaction, as evidenced by comparison with CAM5-FV and the multi-model mean in Blackburn et al. (2013). The climatic state in GRIST-CAM5phys is similar to CAM5-FV and other models. The difference in tropical large-scale precipitation between GRIST-CAM5phys and CAM5-FV sheds light on the role of different physics-dynamics interactions in the two models. The circulation statistics (mean state and transient eddies) obtained by using the CAM5 package is quite similar to the one using the simple physics package (Zhang et al. 2020).

In summary, the CAM5 parameterization suite is successfully transferred and assimilated in the GRIST model framework via the two-step approach. The transferred package shows reasonable behavior in the full physics-dynamics interaction. The SCM is helpful for coupling a sophisticated physics package to a new model system. It reduces the uncertainties during the transfer, and helps to evaluate the model physics in the absence of 3D model dynamics, thus filling the gap for coupling physics to dynamics.

Code and data availability. GRIST is available at https://github.com/grist-dev, in private repositories. The source code is available to a member of the model development projects, or people who have interest. Per the current policy on code sharing at Chinese Academy of Meteorological Sciences, public authorization may be granted provided that one accepts the terms and conditions: https://github.com/GRIST-Dev/TermsAndConditions. A way is provided to the Editor and Reviewer to access the code, which does not compromise their anonymity. A frozen version of the model code and running scripts for supporting this manuscript are available at: https://zenodo.org/record/3960489 (restricted accessed). The isolated CAM5 package, together with its associated datasets and namelist, are available at: https://zenodo.org/record/3960481 (freely accessed). The input and output data of SGRIST1.0 are located at : https://zenodo.org/record/3960487 (freely accessed). The grid data are located at https://zenodo.org/record/3668915 (freely accessed). The CAM5 and SCAM used in this study are part of the CESM1.2, which can be found at : https://www.cesm.ucar.edu/models/cesm1.2/.

Supplement. Supplement.pdf contains Figure S1.

Author contributions. X. Li developed SGRIST1.0, tested and verified the CAM5 parameterization package, with contributions from X. Peng. Y. Zhang created the interface for incorporating CAM5 physics and maintained the workflow of GRIST, with contributions from X. Li., X. Peng and J. Li. X. Li and Y. Zhang inject materials and contents for this manuscript with contributions from X. Peng and J. Li. All the authors continuously discussed the model development and the results of this manuscript.

Competing interests. The authors declare that they have no conflict of interest.

Acknowledgments. This study is supported by the National Key R&D Programs of China on the Monitoring, Early Warning and Prevention of Major Natural Disasters (No. 2018YFC1507005 and No. 2017YFC1502202), the Chinese Academy of Meteorological Sciences Research Project Funds (No. 2019Y002).

References

Ackerman, A. S., Margreet, C, Stevens, B, et al.: Large-eddy simulations of a drizzling, stratocumulus-topped marine boundary layer, Mon. Wea. Rev., 137, 1083–1110, 2009.

Bretherton, C.S. and Park, S.: A new moist turbulence parameterization in the Community Atmosphere Model, J. Clim., 22, 3422–3448, 2009.

Blackburn, M. and Hoskins, B. J.: Context and aims of the Aqua-Planet Experiment, J. Meteor. Soc. Japan, 91, 1–15, 2013.

Davies, L., Jakob, C., Cheung, K., et al.: A single-column model ensemble approach applied to the TWP-ICE experiment, J. Geophys. Res. Atmos., 118, 6544–6563, 2013.

Gates, W. L.: AMIP: The Atmospheric Model Intercomparison Project, Bull. Am. Meteorol. Soc., 73, 1962–1970, 1992.

Gates, W. L., Boyle, J. S., Covey, C., et al.: An overview of the results of the Atmospheric Model Intercomparison Project (AMIP I), Bull. Am. Meteorol. Soc., 80, 29–55, 1999.

Gettelman, A. and Morrison, H.: Advanced two-moment bulk microphysics for global models. Part I: Off-line tests and comparison with other schemes, J. Climate, 28(3), 1268–1287, 2015.

Gettelman, A., Truesdale, J. E., Bacmeister, J. T., et al.: The Single Column Atmosphere Model version 6 (SCAM6): Not a scam but a tool for model evaluation and development, J. Adv. Model. Earth Syst., 11, 1381–1401, 2019.

Guo, Z., Wang, M., Qian, Y., Larson, V. E., et al.: A sensitivity analysis of cloud properties to CLUBB parameters in the Single-Column Community Atmosphere Model (SCAM5), J. Adv. Model. Earth Syst., 6, 829–858, 2014.

Gross, M, Wan, H., Rasch, P. J., et al.: Physics-dynamics coupling in weather, climate, and earth system models: challenges and recent progress, Mon. Wea. Rev., 146, 3505–3544, 2018.

https://doi.org/10.5194/gmd-2020-254
Preprint. Discussion started: 12 October 2020

Hack, J. J. and Pedretti, J. A.: Assessment of solution uncertainties in single-column modeling frameworks, J. Climate, 13(2), 352-365, 2000.

Herrington, A. R. and Reed, K. A.: An idealized test of the response of the Community Atmosphere Model to near-grid-scale forcing across hydrostatic resolutions, J. Adv. Model. Earth Syst., 10, 560– 575, 2017.

Holland, J. Z. and Rasmusson, E. M.: Measurement of atmospheric mass, energy, and momentum budgets over a 500-kilometer square of tropical ocean, Mon. Wea. Rev., 101, 44–55, 1973.

Iacono, M., Delamere, J., Mlawer, E., et al: Radiative forcing by long-lived greenhouse gases: Calculations with the AER radiative transfer models, J. Geophys. Res., 113, D13103, 2008.

Jablonowski, C., Lauritzen, P. H., Nair, R. D., and Taylor, M.: Idealized test cases for the dynamical cores of Atmospheric General Circulation Models: A proposal for the NCAR ASP 2008 summer colloquium, available online: http://www-personal.umich.edu/~cja-blono/DCMIP-2008_TestCaseDocument_29May2008.pdf., 2008.

Klein, S. A., McCoy, R. B., Morrison, H., et al.: Intercomparison of model simulations of mixed-phase clouds observed during the ARM Mixed-Phase Arctic Cloud Experiment. I: Single-layer cloud, Q. J. R. Meteorol. Soc., 135(641), 979-1002, 2009.

Li, X. H., Peng, X. D., and Zhang, Y.: Investigation of the effect of the time step on the physics–dynamics interaction in CAM5 using an idealized tropical cyclone experiment, Climate Dyn., available online: https://doi.org/10.1007/s00382-020-05284-5, 2020.

Liang, X. Z. and Wang, W. C.: Atmospheric ozone climatology for use in General Circulation Models. PCMDI Report No. 43: UCRL-MI-125650, 25 pp, 1996, Accessible online at https://pcmdi.llnl.gov/mips/amip/AMIP2EXPDSN/OZONE/ OZONE2/o3wangdoc.html.

Lin, S. J.: A "vertically Lagrangian" finite-volume dynamical core for global models, Mon. Wea. Rev., 132, 2293–2307, 2004.

May, P. T., Mather, J. H., Vaughan, G., and Jakob, C.: Characterizing oceanic convective cloud systems: The Tropical Warm Pool International Cloud Experiment, Bull. Amer. Meteor. Soc., 89(2), 153–155, 2008.

Moncrieff, M. W., Krueger, S. K., Gregory, D., et al.: GEWEX Cloud System Study (GCSS) working group 4: Precipitating convective cloud systems, Bull. Amer. Meteor. Soc., 78, 831–845, 1997.

https://doi.org/10.5194/gmd-2020-254
Preprint. Discussion started: 12 October 2020

Morrison, H. and Gettelman, A.: A new two-moment bulk stratiform cloud microphysics scheme in the Community Atmosphere Model, version 3 (CAM3). Part I: Description and numerical tests, J. Climate, 21, 3642–3659, 2008.

Neale, R. B. and Hoskins, B. J.: A standard test for AGCMs including their physical parametrizations. I: The proposal, Atmos. Sci. Lett., 1, 101–107, 2000.

Neale, R. B., Richter, J. H., and Jochum, M.: The impact of convection on ENSO: From a delayed oscillator to a series of events, J. Climate, 21, 5904–5924, 2008.

Neale, R. B., Chen, C. C., Getteman, A., et al: Description of the NCAR Community Atmosphere Model (CAM 5.0). NCAR Technical Note. NCAR/TN-486+STR, pp 108–117, 2010.

Neggers, R. A. J., Siebesma, A. P., and Heus, T.: Continuous single-column model evaluation at a permanent meteorological supersite, Bull. Amer. Meteor. Soc., 93, 1389–1400, 2012.

Neggers, R. A. J.: Attributing the behavior of low-level clouds in large-scale models to subgrid-scale parameterizations, J. Adv. Model. Earth Syst., 7, 2029–2043, 2015.

Park, S. and Bretherton, C. S.: The University of Washington shallow convection and moist turbulence schemes and their impact on climate simulations with the Community Atmosphere Model, J. Climate, 22, 3449–3469, 2009.

Park, S., Bretherton, C. S., and Rasch, P. J.: Integrating cloud processes in the Community Atmosphere Model, version 5, J. Climate, 27, 6821–6855, 2014.

Randall, D. A., Xu, K. M., Somerville, R. J. C., and Iacobellis, S.: Single-column models and cloud ensemble models as links between observations and climate models, J. Climate, 9(8), 1683–1697, 1996.

Randall, D. A., Krueger, S., Bretherton, C., et al.: Confronting models with data: The GEWEX cloud systems study, Bull. Amer. Meteor. Soc., 84, 455–469, 2003.

Reed, K. A. and Jablonowski, C.: An analytic vortex initialization technique for idealized tropical cyclone studies in AGCMs, Mon. Wea. Rev., 139, 689–710, 2011a.

Reed, K. A. and Jablonowski, C.: Assessing the uncertainty in tropical cyclone simulations in NCAR's Community Atmosphere Model, J. Adv. Model. Earth Syst., 3: MS000076, 2011b.

Reed, K. A. and Jablonowski, C.: Idealized tropical cyclone simulations of intermediate complexity: A test case for AGCMs, J. Adv. Model. Earth Syst., 4, M04001, 2012.

https://doi.org/10.5194/gmd-2020-254
Preprint. Discussion started: 12 October 2020

Geoscientific Model Development Discussions

Ringler, T. D., Thuburn, J., Klemp, J. B., and Skamarock, W. C.: A unified approach to energy conservation and potential vorticity dynamics for arbitrarily-structured C-grids. Journal of Computational Physics, 229(9), 3065–3090, 2010.

Siebesma, A. P., Bretherton, C.S., Brown, A., et al.: A large eddy simulation intercomparison study of shallow cumulus convection, J. Atmos. Sci., 60, 1201–1219, 2003.

Skamarock, W. C. and Gassmann A.: Conservative transport schemes for spherical geodesic grids: High-order flux operators for ODE- based time integration, Mon. Wea. Rev., 139, 2962–2975, 2011.

Stevens, B., Lenschow, D. H., Vali, G., et al.: Dynamics and chemistry of marine stratocumulus DYCOMS-II, Bull. Amer. Meteor. Soc., 84(5), 579–594, 2003.

Thatcher, D. R. and Jablonowski, C.: A moist aquaplanet variant of the Held-Suarez test for atmospheric model dynamical cores, Geosci. Model Dev., 9, 1263–1292, 2016.

Thuburn, J., Ringler, T. D., Skamarock, W. C., and Klemp, J. B.: Numerical representation of geostrophic modes on arbitrarily structured C-grids. Journal of Computational Physics, 228(22), 8321–8335, 2009.

Ullrich, P. A., Jablonowski, C., Kent, J., Lauritzen, P. H., Nair, R. D., and Taylor, M. A.: Dynamical core model intercomparison project (DCMIP) test case document, Tech. rep., 2012.

Ullrich, P. A., Jablonowski, C., Kent, J., et al: DCMIP2016: a review of non-hydrostatic dynamical core design and intercomparison of participating models, Geosci. Model Dev., 10, 4477–4509, 2017.

Wang, L., Zhang, Y., Li, J., et al.: Understanding the Performance of an Unstructured-Mesh Global Shallow Water Model on Kinetic Energy Spectra and Nonlinear Vorticity Dynamics, J. Meteor. Res., 33, 1075–1097, 2019.

Wicker, L. J. and Skamarock, W. C.: Time-splitting methods for elastic models using forward time schemes, Mon. Wea Rev., 130, 2088–2097, 2002.

Xie, S., Hume, T., Jakob, C., et al.: Observed large-scale structures and diabatic heating and drying profiles during TWP-ICE, J. Climate, 23, 57–79, 2010.

Yu, R. C., Zhang, Y., Wang, J. J., et al: Recent progress in numerical atmospheric modeling in China, Adv. Atmos. Sci., 36(9), 938–960, 2019.

https://doi.org/10.5194/gmd-2020-254
Preprint. Discussion started: 12 October 2020

Zhang, G. J. and McFarlane, N. A.: Sensitivity of climate simulations to the parameterization of cumulus convection in the Canadian Climate Centre general circulation model, Atmos Ocean, 3, 407–446, 1995.

Zhang, M., Bretherton, C. S., Blossey, P. N., et al.: CGILS: Results from the first phase of an international project to understand the physical mechanisms of low cloud feedbacks in single column models, J. Adv. Model. Earth Syst., 5, 826–842. 2013.

Zhang, M., Somerville, R. C. J., and Xie, S. C.: The SCM concept and creation of ARM forcing datasets. Meteorological Monographs, 57, 24.1–24.12, 2016.

Zhang, Y., Yu, R., and Li, J.: Implementation of a conservative two-step shape-preserving advection scheme on a spherical icosahedral hexagonal geodesic grid, Adv. Atmos. Sci., 34(3), 411–427, 2017.

Zhang, Y.: Extending high-order flux operators on spherical icosahedral grids and their applications in the framework of a shallow water model, J. Adv. Model. Earth Syst., 10, 145–164, 2018.

Zhang, Y., Li, J., Yu, R. C., et. al.: A Layer-Averaged Nonhydrostatic Dynamical Framework on an Unstructured Mesh for Global and Regional Atmospheric Modeling: Model Description, Baseline Evaluation, and Sensitivity Exploration, J. Adv. Model. Earth Syst., 11, 1685-1714, 2019.

Zhang, Y., Li, J., Yu, R. C., et al: A Multiscale Dynamical Model in a Dry-Mass Coordinate for Weather and Climate Modeling: Moist Dynamics and Its Coupling to Physics, Mon. Wea. Rev., 148, 2671-2699, 2020.

https://doi.org/10.5194/gmd-2020-254
Preprint. Discussion started: 12 October 2020

Table 1. A list of resolution and time step sizes used in the tropical cyclone experiment

Resolution	Averaged spherical grid distance	Dry core time step	tracer time step	Examined model (physics) time step (dt)			
G6	~120 km	300 s	600 s		600 s	1200 s	2400 s
G7	~60 km	150 s	300 s	300 s	600 s	1200 s	2400 s
G8	~30 km	75s	150 s	300 s	600 s	1200 s	

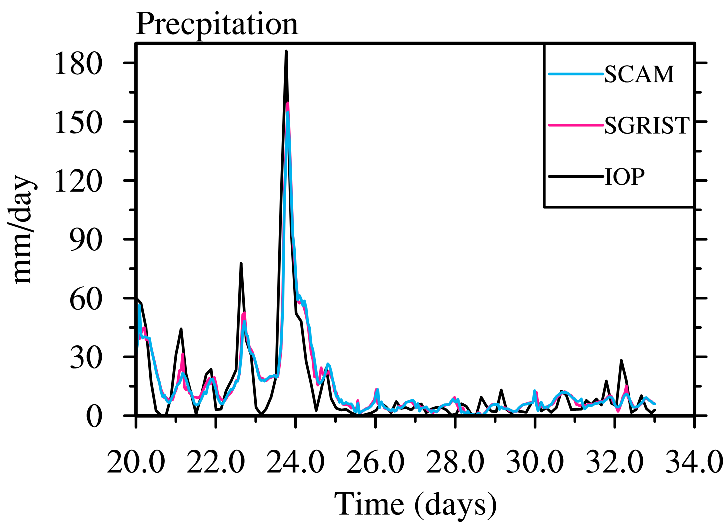

Figure 1. Time series of precipitation rate in the TWP-ICE test case from the SGRIST1.0 (red line) and SCAM (blue line) simulations and the IOP data (black line), mm day^{-1}.

https://doi.org/10.5194/gmd-2020-254
Preprint. Discussion started: 12 October 2020

Geoscientific Model Development Discussions
Open Access
EGU

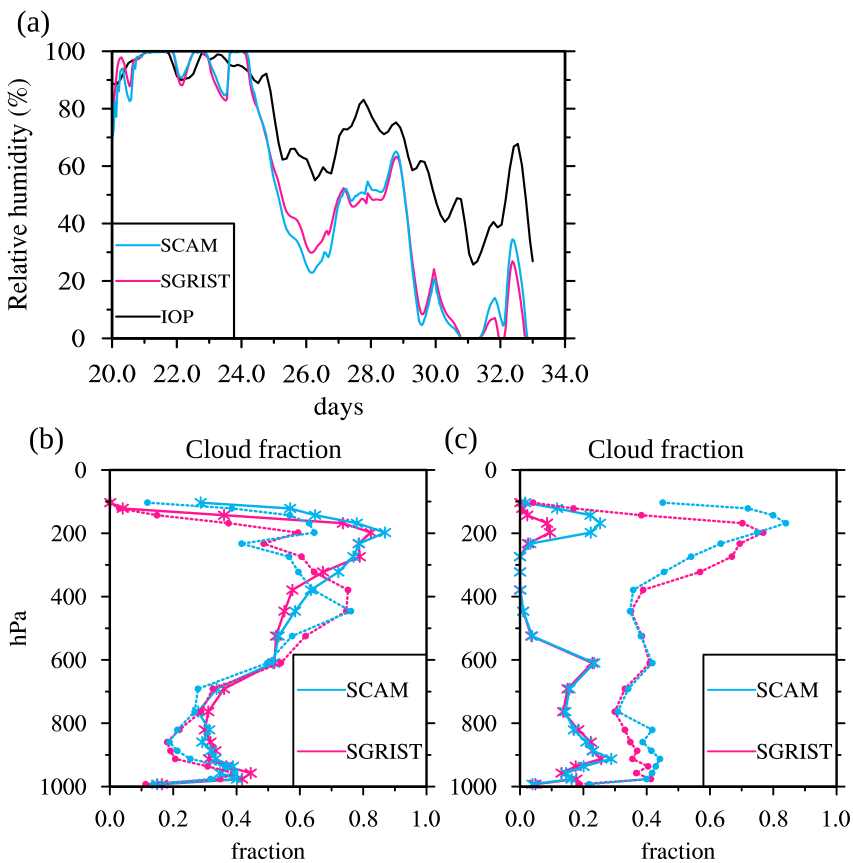

577

578 **Figure 2.** (a) Time series of relative humidity, %, at 500 hPa in the SGRIST1.0 (red line) and SCAM

579 (blue line) simulations and the IOP data (black line). Period-averaged cloud fraction for the (b)

580 convection active period and (c) suppressed period in the SGRIST1.0 and SCAM simulations with *dt*

581 = 1200 (solid lines) and 2400s (dotted lines).

582

583

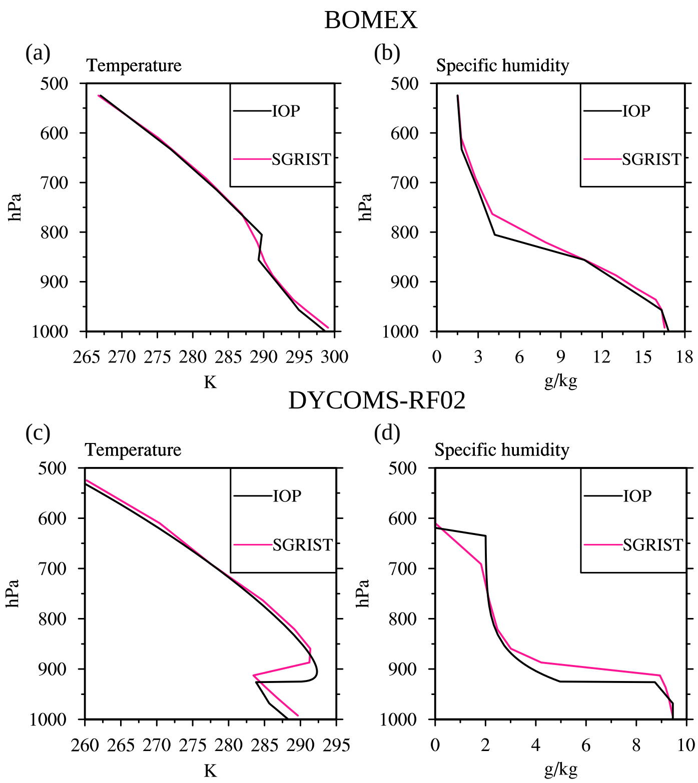

Figure 3. Comparison of the temperature and specific humidity between the initial condition from the IOP data (black lines) and the time-average profiles in SGRIST1.0 (red lines) for (a, b) the BOMEX test case and (c, d) the DYCOMS-RF2 test case. The last 3-hour average of SGRIST1.0 is shown in the BOMEX case and the last 5-hour average is shown in the DYCOMS-RF2.

https://doi.org/10.5194/gmd-2020-254
Preprint. Discussion started: 12 October 2020

Geoscientific Model Development
Discussions

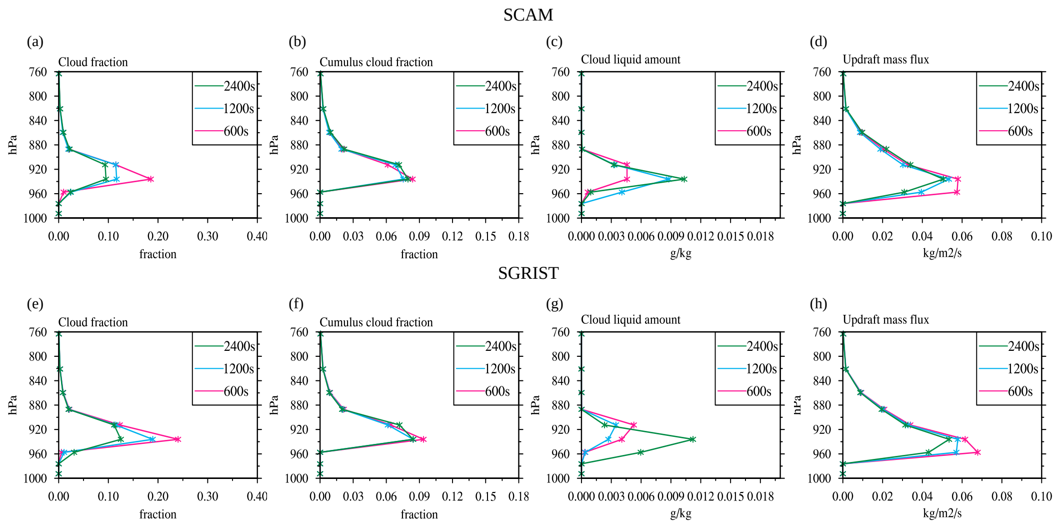

Figure 4. Time-average of cloud fraction, cumulus cloud fraction, cloud liquid amount, g kg^{-1}, and updraft mass flux, kg m^{-2} s^{-1}, over the last 3-hour simulations in the BOMEX test case using (a-d) SCAM and (e-h) SGRIST1.0 with *dt* = 600, 1200, and 2400 s.

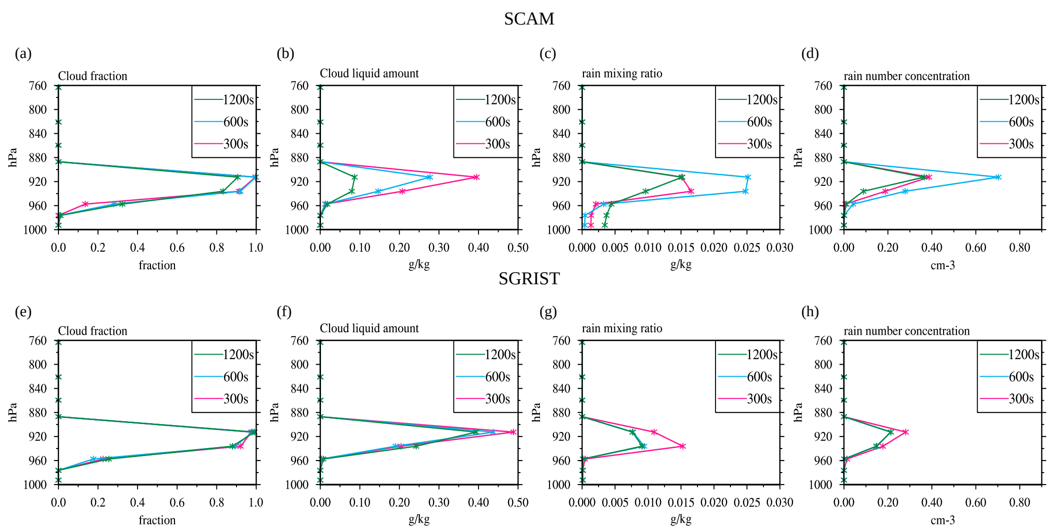

Figure 5. Time-average of cloud fraction, cloud liquid amount, g kg^{-1}, rain mixing ratio, g kg^{-1}, and rain number concentration, cm^{-3}, over the last 5-hour simulations in the DYNCOMS-RF02 test case using (a-d) the SCAM and (e-h) the SGRIST1.0 models with *dt* = 300, 600 and 1200 s.

https://doi.org/10.5194/gmd-2020-254
Preprint. Discussion started: 12 October 2020

Geoscientific Model Development
Discussions

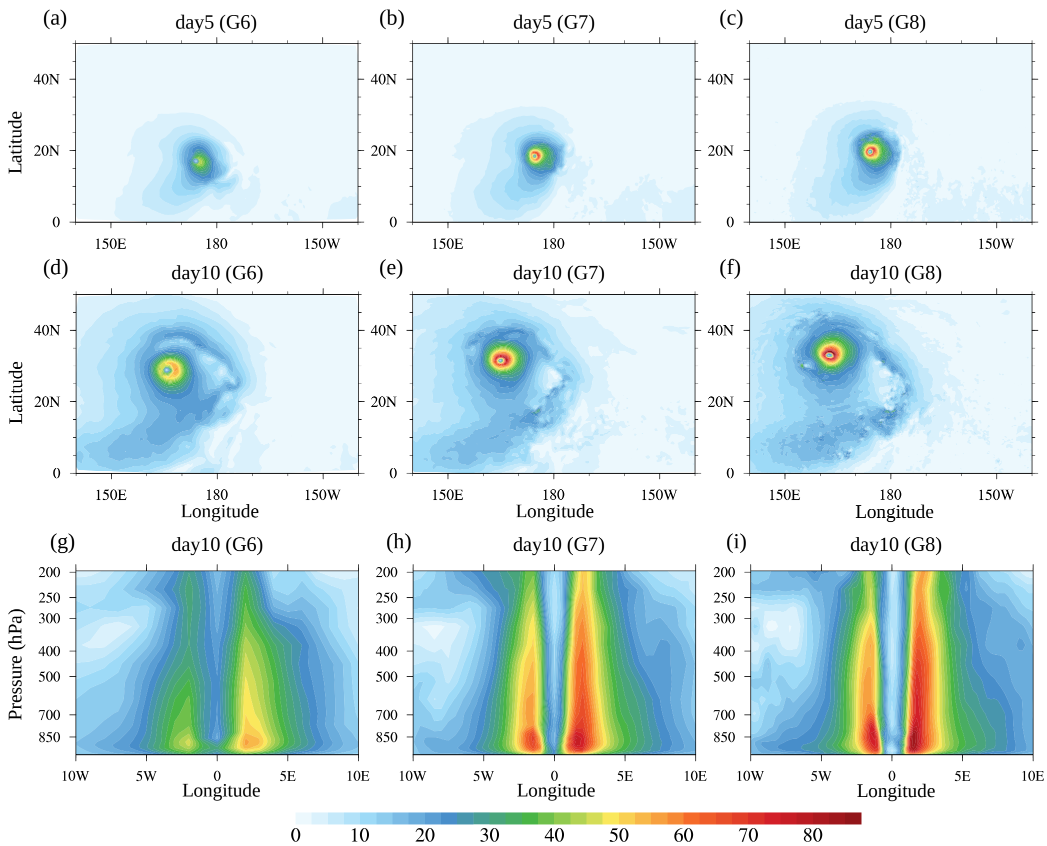

Figure 6. Snapshot of the simulated storm at days 5 and 10 for ptend_f2_sudden configuration in GRIST-CAM5phys at G6, G7 and G8 resolutions, m s^{-1}. The model time steps are 1200s for G6, 600s for G7, and 300s for G8 resolutions. Wind speed at 850 hPa on (a-c) day 5 and (d-f) day 10, and (g-i) height-longitude cross-sections of the wind speed through the center latitude of the storm on day 10.

https://doi.org/10.5194/gmd-2020-254
Preprint. Discussion started: 12 October 2020

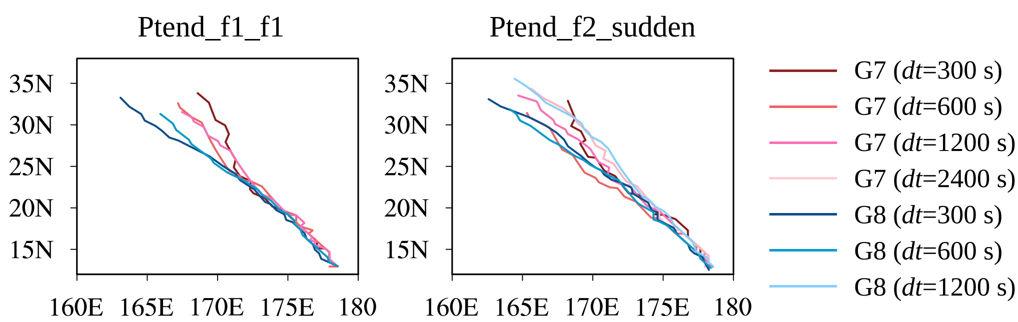

Figure 7. The path of the storm center from day 2 to day 10 in the ptend_f1_f1 and ptend_f2_suddden simulations at G7 and G8 resolutions.

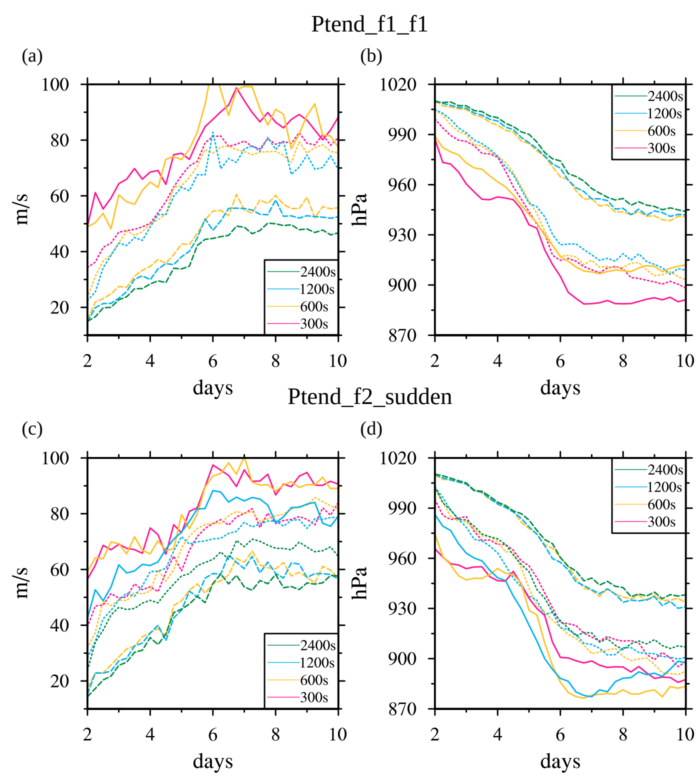

Figure 8. The temporal evolution of maximum wind speed at 850 hPa, m s^{-1}, and minimum surface pressure, hPa, for (a and b) the ptend_f1_f1 and (c and d) ptend_f2_sudden simulations at G6 (dashed lines), G7 (dotted lines), and G8 (solid lines) resolutions.

https://doi.org/10.5194/gmd-2020-254
Preprint. Discussion started: 12 October 2020

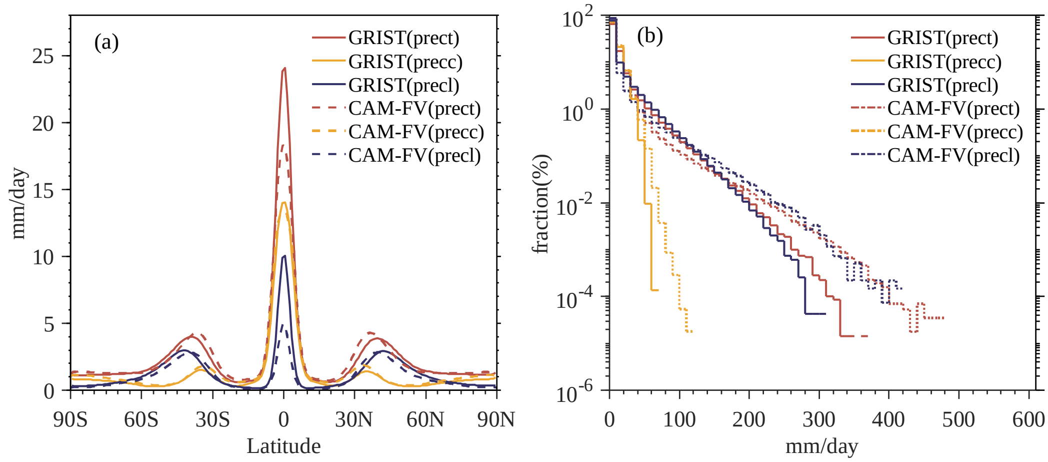

Figure 9. (a) Zonal-time average of total (prect), convective (precc), and large-scale precipitation (precl), mm day^{-1}, in the APE simulations of GRIST-CAM5phys and CAM5-FV. (b) Frequency distribution of daily precipitation within 10° S-10° N in bins of a10 mm day^{-1} width, with precipitation less than 0.5 mm day^{-1} being omitted.

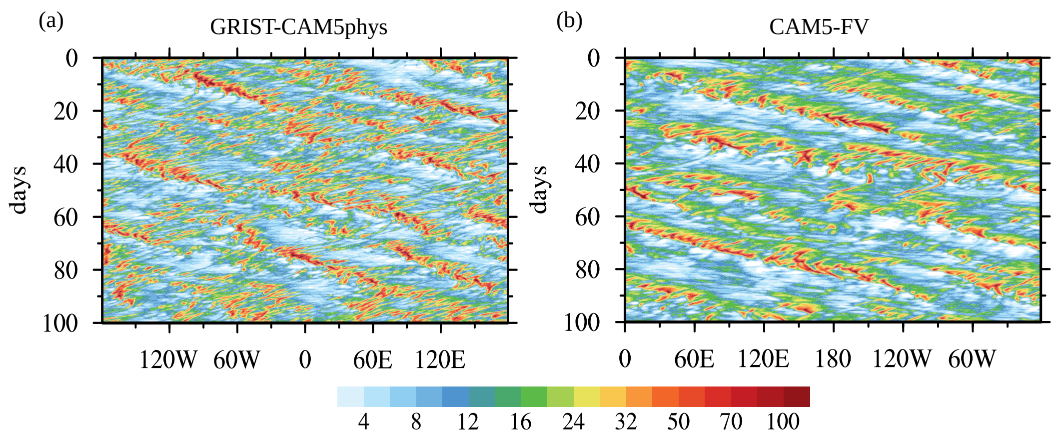

Figure 10. Hovmöller plots of the area-averaged precipitation between 5° S and 5° N for an arbitrary 100-day period of the APE simulations of GRIST-CAM5phys and CAM5-FV, mm day^{-1}.

https://doi.org/10.5194/gmd-2020-254
Preprint. Discussion started: 12 October 2020

Geoscientific Model Development
Open Access
Discussions
EGU

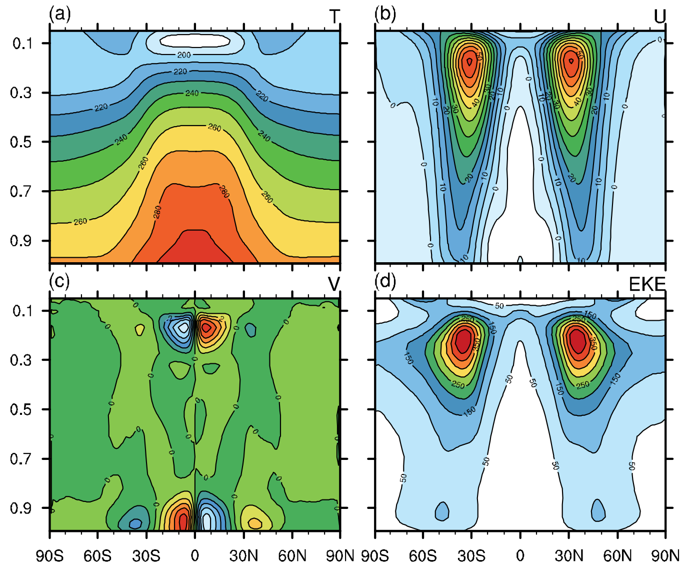

Figure 11. Zonal-time average of (a) temperature (*T*), K, (b) zonal wind (*U*), m s^{-1}, (c) meridional wind (*V*), m s^{-1}, and (d) eddy kinetic energy (*EKE*), m^{-1} s^{-1}, for the GRIST-CAM5phys APE simulation.